ChemPubSoc Europe

DOI: 10.1002/cptc.201900093

CHEMPHOTOCHEM Articles

All-Optical Temperature Sensing in Organogel Matrices via Annihilation Upconversion

Nadzeya Nazarova,[a] Yuri Avlasevich,[a] Katharina Landfester,*[a] and Stanislav Baluschev*[a, b]

Modified organogels are bicontinuous colloidal systems which form a three-dimensional network embedding well-solvated organic dyes sensitive to minor changes in its microenvironment. It was demonstrated that these natural wax/oils based organogels can be applied for minimally invasive temperature sensing in life-science objects. The desired temperature sensitivity of better than 100 mK, centered around the physiologically relevant temperature of 36 °C, is warranted by using the process of triplet-triplet annihilation photon energy upconversion (TTA-UC) as a sensing mechanism. This all-optical sensing technique, based on ratiometric-type signal registration, ensures significant independence of the data obtained on excitation intensity instabilities, local molecular concentration fluctuations and field-of-view variations. The TTA-UC system is effectively protected for more than 1000 s against oxygen-induced damage, allowing stable performance of this temperature-sensing system even in ambient environments without lost of sensitivity and applying the same calibration curve.

1. Introduction

The materials used for additive manufacturing (bioprinting) should be biocompatible, biodegradable, and should not have any toxic effect, which should also include both their waste compounds and intermediates.[1,2] Organogels can be considered as bicontinuous colloidal systems that coexist as a micro-heterogeneous solid and a liquid phase.[3] Organogels, used as bio-inks, can be used to broaden the technology portfolio of the 3D bioprinting adding potential for the creation of sensing tools which are compatible with the created organic objects.

A number of critical reviews have summarized the progress in biocompatible T-measurements. There is a broad consensus that optical methods for T-sensing are less invasive and able to provide the time-resolved and 2-dimensional spatial evolution of the T-distribution.[4–8] As an example for the huge amount of works, dealing with T-sensing in life-science objects one can mention the systems using nanogels, luminescent CdSe-CdS quantum dots as donors and cyanine dyes as acceptors, dual-emitting nanoparticles, fluorescence polarization anisotropy of green fluorescent proteins.[9–12] A common characteristic for these systems is the ratiometric T-response achieved, where the luminescence of one of the species does not depend on the temperature, but the other depends strongly on the temperature.

As a consequence of temperature increase, both the phosphorescence intensity and phosphorescence lifetime decrease which often is used for all-optical temperature sensing. Temperature is known to influence: (a) the phosphorescence quantum yield (QY) of the used dye; (b) the quenching constant(s); (c) the solubility of oxygen; (d) the diffusion of oxygen; and (e) the temperature change facilitates singlet-triplet and triplet-singlet transitions.[6] In the presence of molecular oxygen, the energy stored in the triplet ensemble excited states is being actively dissipated, which competes with emissive (phosphorescence) or non-emissive (triplet-to-triplet) energy transfer processes. This is as a result of efficient energy transfer between the organic molecule's triplet state and the ground state of molecular oxygen, leading to the formation of singlet oxygen (marked as S_1 ($^1\Delta_g$); Figure 1). Singlet oxygen is a particularly reactive species which can oxidize the photoactive molecules leading to a further loss of efficiency. Herein we report an approach to assembling a fully biocompatible temperature sensitive organogel system, where the material temperature response is obtained in an all-optical manner.

2. Advantages of Temperature Sensing using an Organogel-Based TTA-UC System

2.1. TTA-UC Process in an Organogel Matrix

The lateral spatial resolution of the proposed sensing method depends only on the size and intensity distribution of the testing optical field (diffraction limited). Special attention deserves the fact, that the testing optical schema is based on the technique of ratiometric optical registration, thus allowing to reveal absolute temperature distribution of the studied

[a] N. Nazarova, Dr. Y. Avlasevich, Prof. K. Landfester, Dr. S. Baluschev
Max Planck Institute for Polymer Research
Mainz 55128 (Germany)
E-mail: landfest@mpip-mainz.mpg.de
[b] Dr. S. Baluschev
Optics and Spectroscopy Department
Faculty of Physics
Sofia University "Saint Kliment Ochridski"
Sofia 1164 (Bulgaria)
E-mail: balouche@phys.uni-sofia.bg

Supporting information for this article is available on the WWW under https://doi.org/10.1002/cptc.201900093

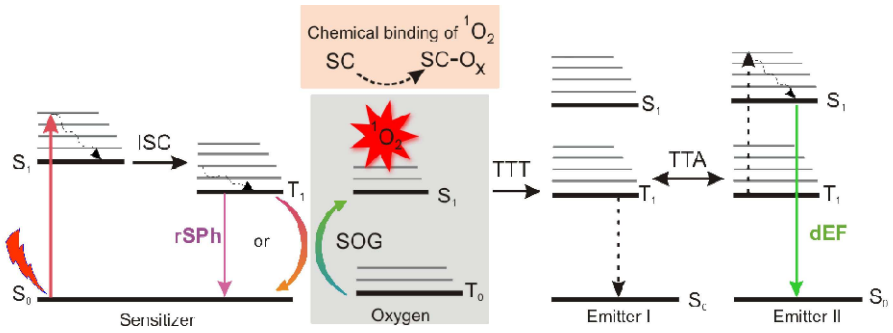

Figure 1. Simplified energetic scheme of the triplet-triplet annihilation upconversion process in an oxygen rich environment, containing singlet oxygen scavenging moieties. Abbreviations: SOG = singlet oxygen scavenger; rSPh = residual sensitizer phosphorescence; dEF = delayed emitter fluorescence.

object both, in space (creating 2D-temperature map) and in time (visualizing the temporal evolution).[13]

The desired temperature sensitivity, biocompatibility and reproducibility of the reported here technology is warranted by using the triplet-triplet annihilation photon energy upconversion process (TTA-UC), realized in fully biocompatible soft matter matrix as an all-optical sensing tool.

In Figure 1 is shown the simplified energetic scheme of the TTA-UC process, which takes place in a multi-chromophore hydrophobic system consisting of energetically optimized pairs of sensitizer (metallated macrocycles) and emitter molecules (aromatic hydrocarbons).[14] The photon energy is absorbed at the sensitizer singlet manifold (the red arrow, Figure 1) and stored in its triplet state formed in the process of intersystem crossing (ISC). Next, via the process of triplet-triplet transfer (TTT) the accumulated energy is transferred to an emitter triplet state. Further, the excited triplet states of two emitter molecules undergo triplet-triplet annihilation (TTA), in which one emitter molecule returns back to its singlet ground state and the other molecule gains the energy of both triplet states and is excited to the higher singlet state. As the emitter singlet state decays radiatively back to the ground state, a delayed emitter fluorescence (the green arrow, Figure 1, called shortly dEF), bearing higher energy than that of the excitation photon, is emitted. Simultaneously, if the energy overlap between the triplet manifolds of the emitter and sensitizer molecules is not optimal or the rotational diffusion of the interacting sensitizer/emitter triplet states is not optimal, the sensitizer triplet state will not be completely depopulated and therefore residual sensitizer phosphorescence (the violet arrow, Figure 1, called shortly rSPh) will be observed.[15,16]

Thus, to fully demonstrate the critical advantages of the TTA-UC process used as a T-sensing all-optical tool, the development of an effective protection strategy against quenching by molecular oxygen and protection against the subsequent production of highly reactive singlet oxygen is essential.[17] All these requirements are fulfilled when the TTA-UC process is performed in hydrophobic matrices such as blends of natural waxes/oils with pronounced singlet oxygen scavenging properties. This approach ensures simultaneously the ability to tune the T-sensitivity towards biologically relevant temperature window (centered at T = 36 °C), to use effectively singlet oxygen scavenging properties of the natural oils and last, but not least to apply hereditary biocompatible materials (all used waxes/oils are approved as food additives).

In presence of molecular oxygen dissolved at the wax/oil sample, during the optical excitation singlet oxygen is generated continuously. The phytochemical compounds of the vegetable oils (for example, tocopherol, tocotrienol and γ-oryzanol) demonstrate remarkable activity to bind chemically all present amounts of singlet oxygen.[18] Since the oxygen permeation rate through the samples surface is much lower than the rate of chemical binding of singlet oxygen, after a short initial period, the whole oxygen content is consumed. This fact is manifested by the actually stationary intensity of the TTA-UC signal, demonstrated at Figure 1. Waxes are complex mixtures of a number of non-polar and polar components, such as hydrocarbons, esters, fatty acids and fatty alcohols with varying carbon chain lengths. Natural waxes are considered to be the most effective gelators for vegetable oils.[19] Moreover, the gels formed using waxes have demonstrated very high thermal reversibility, i.e. no spontaneous phase separation was observed.

Hydrogen bonding between the molecules in the wax-oil network could be weakened by heating that leads to changes into the intermolecular interactions between the UC-dyes and matrix environment in the organogel. As a result, the efficiency of the TTA-UC process depends strongly on the organogel temperature.

2.2. Temperature Sensing Procedure

The temperature sensing method performed in bio-compatible organogel matrix is elucidated in Figure 2. This ratiometric-type sensing technique is based on dual-signal response of the TTA-UC system embedded in organogel matrix: it was demonstrated that at specific experimental conditions (optimally chosen energy positions of the interacting sensitizer and emitter triplet states, singlet oxygen scavenging ability and properly tuned viscosity of the hydrophobic matrix) the dEF (Figure 2 a, emission spectra around central wavelength of λ = 520 nm) and rSPh (Figure 2 a, emission spectra around central wavelength of λ = 795 nm) are comparable – i.e. both registered optical signals have comparable intensity. As rule of thumb, if the viscosity of the hydrophobic matrix, embedding the TTA-UC system increases, the intensity of

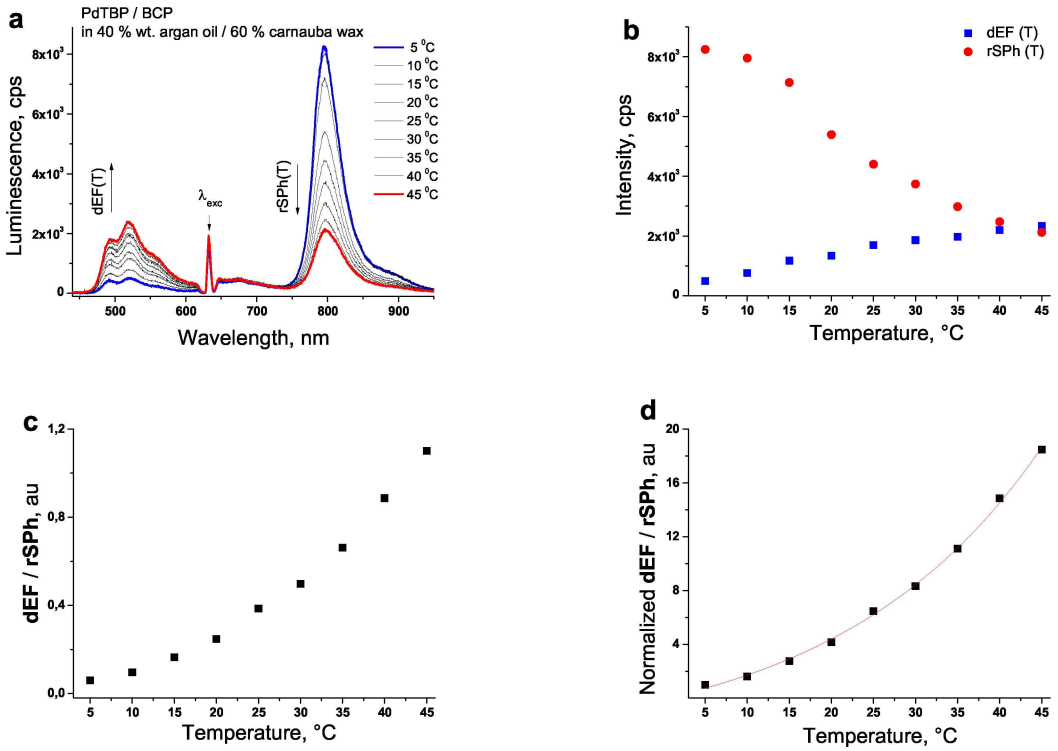

Figure 2. Procedure allowing all-optical and ratiometric local temperature sensing via biocompatible organogel-based TTA-UC system. (a) Luminescence spectra of the studied TTA-UC system consisting of PdTBP/BCP in 40% wt. argan oil/60% carnauba wax; (b) Temperature dependence of the signals of dEF (blue squares) and rSPh (red circles); (c) Dependence of the ratio dEF/rSPh on local temperature; (d) Normalization of the ratio dEF/rSPh regarding the value for $T = 5°$. The red curve is an exponential fit of the experimental points.

the dEF decreases, simultaneously the intensity of the rSPh increases. This simple rule is valid only, if the sample is oxygen free. This similarity of the intensities of the optical signals ensures stable and simple registration, because no additional filters are necessary.

Quasi oxygen-free operation of the TTA-UC system could be achieved even if the sample is placed and kept in ambient environment (oxygen content > 20% O_2 vol.) if the diffusion of the molecular oxygen, dissolved at the hydrophobic matrix throughout the borders of the optically assessed spot is much slower than the rate of consumption (chemical bonding) of the singlet oxygen inside this optical spot. For instance, in Figure 3 are demonstrated the temporal dependences of the intensity of the optical signals of dEF (the blue line) and rSPh (the red line) for constant excitation intensity of $I_{exc} = 20\ mW\,cm^{-2}$, wavelength $\lambda = 635$ nm achieved from temperature stabilised *cw*-diode laser. The optical excitation begins at $t_1 = 5$ s: it is evident, that at $t_2 = 20$ s the signals of dEF and rSPh are enough stable, i.e. across the excitation spot the concentration of unbounded molecular oxygen is very low, therefore, the signals of dEF and rSPh are not significantly changed and can be used further as measure for the local temperature.

At the following a multidimensional optimization process for the materials parameters leading to the ability of all-optical and local sensing of the temperature within the biologically relevant window (placed surround central temperature of $T_C = 36\,°C$) will be described.

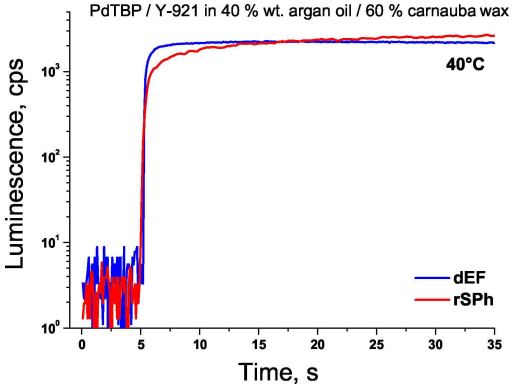

Figure 3. Time dependence of the intensity of the optical signals of dEF (blue line) and rSPh (red line) for the TTA-UC system (presented in Figure 2). Experimental conditions for all measurements: Ambient environment (O_2 > 20% vol.); sample temperature = 40 °C, the temperature is 40°C or did you mean sample temperature = −40 °C.

3. Results

3.1. Selecting Parameters to Optimize Organogel Matrices

Mobility of the dye molecules dispersed at the organogel depends significantly on viscosity of the matrix environment and on the dye-matrix interactions (rotational diffusion of the dye molecules). As first optimization parameter the amphiphilicity of the emitter molecules was altered: the series of emitter

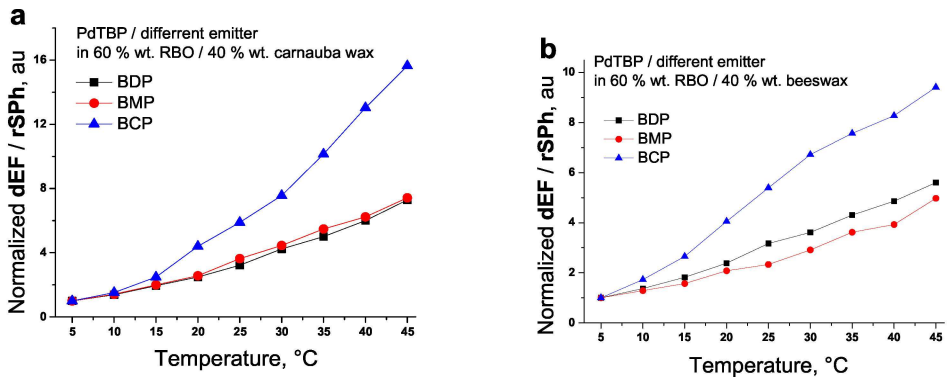

Figure 4. Temperature dependence of the normalized ratio of dEF/rSPh for sensing TTA-UC systems, with varying composition, as follows: (a) Matrix consisting of 60% wt. RBO/40% wt. carnauba wax and different emitters (BDP = black squares, BMP = red circles, BCP = blue triangles); (b) Matrix consisting of 60% wt. RBO/40% wt. beeswax and different emitters (BDP = black squares, BMP = red circles, BCP = blue triangles). For all measurements the same sensitizer PdTBP was used. The spectra are obtained at the $t = 15$ s after the start of the optical excitation.

molecules 3,10-bis(3,3-dimethylbutyn1-yl) perylene (BDP), 3,9 (10)-bis(3,5-dimethoxyphenyl) perylene (BMP) and 3,4,9,10-tetra (butoxycarbonyl) perylene (BCP) in the order of hydrophobicity decreasing are posted.

As matrix materials allowing significant increase of the molecular rotational diffusion of the optically active molecules for a temperature interval centered at 36 °C were chosen 2 natural waxes – beeswax and carnauba wax. Both are biocompatible and defined as food additives: E901 and E903, correspondingly. Since their melting points, 62–64 °C for beeswax and 82–86 °C for carnauba wax are significantly higher than the central temperature of interest (36° C) it is necessary to use as emollients natural oils.

As emollients three natural materials (rice bran oil, further marked as RBO, peanut oil (PEO) and argan oil (AO)) will be applied. The main reason to use emollients is to lower in controllable manner (by studying wax/oil mixtures with different composition) the melting point of the mixture natural wax/emollient. As a main mechanism for control not the macroscopically melting point will be used, but the increase of the sensitivity of the TTA-UC process on the sample temperature.

3.2. Temperature Sensitivity of Composition-Tunable Organogel Matrices

Since the spectral shape of the dEF signal and the spectral shape of rSPh signal is not changed with the change of the sample temperature, for simplicity, in our study we will use instead integral delayed fluorescence of the emitter the maximal fluorescence intensity at certain wavelength. Similarly, instead of integral residual phosphorescence of the sensitizer, the maximal phosphorescence intensity at certain wavelength will be used.

In Figure 4, temperature dependences of the normalized ratio of dEF/rSPh for sensing TTA-UC systems, with varying compositions are shown. Two parameters, namely the amphiphilicity of emitter molecules together with the wax-type, were varied simultaneously. All other exponential parameters such as excitation intensity (20 mWcm^{-2}), sample thickness (1000 μm), mass ratio between wax/oil (40% wt./60% wt., respectively), type of the oil (RBO), sensitizer (PdTBP) and molar concentration of the sensitizer/emitter couple (1×10^{-5} M/2×10^{-4} M) were kept constant. From Figure 4 it is evident, that for both wax-types the emitter molecule with lowest hydrophobicity (BCP) demonstrates the highest sensitivity to small temperature changes of the matrix temperature.

Figure 5 reveals that TTA-UC system embedded in matrix material based on carnauba wax demonstrates first higher optical signals (especially for the sensitizer phosphorescence) and second, a monotonic increaser of the signal of delayed emitter fluorescence. This fact explains the higher temperature sensitivity for carnauba-based samples. It is worthy to mention, that similar behaviour was observed also by others emitter molecules.

The next optimization step is shown in Figure 6: here the sensitizer and emitter molecules as well as the matrix material with higher melting point (carnauba wax) were not changed. Optimized was only the type of low melting point matrix material.

As evident from Figure 6, the sample containing peanut oil demonstrates the highest temperature sensitivity. The last optimization step includes gradual change of the ratio of percentage by weight matrix material with higher melting point regarding the percentage by weight the matrix material with low melting point. The results are reported in Figure 7 (a). As shown in Figure 7 (a) the TTA-UC sensing composition-PdTBP/BCP in 80% wt. PEO/20% wt. carnauba wax it (the violet triangles) demonstrates highest sensitivity to temperature changes inside the biologically relevant interval around 36 °C.

Even more, this composition shows strongly monotonic increase of the dEF-signal by increasing of the sample temperature (Figure 7 (b), the blue squares), simultaneously with strongly monotonic decrease of the rSPh-signal by rising of sample temperature (Figure 7 (b), the red circles). This experimental fact ensures creation of a non-ambiguous calibration curve linking the measured in all-optical regime the ratio of dEF/rSPh signals and local sample temperature (across the

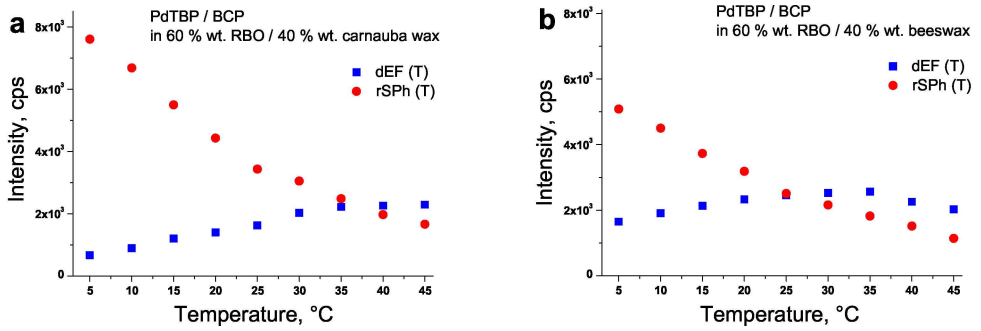

Figure 5. Temperature dependence of the signals of dEF (blue squares) and rSPh (red circles): (a) for TTA-UC systems based on carnauba wax; (b) for TTA-UC systems based on beeswax. The other experimental parameters are the same as in Figure 4.

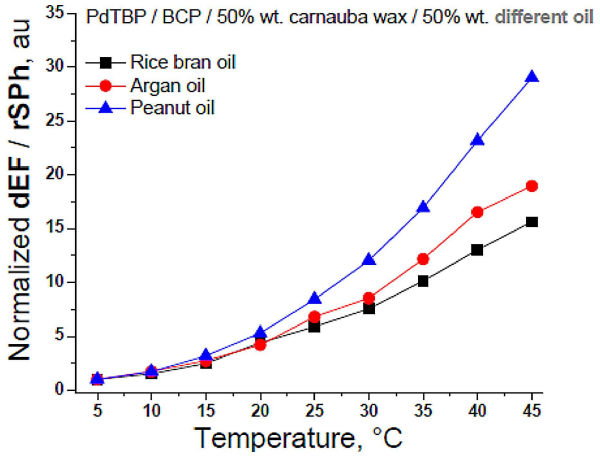

Figure 6. Temperature dependence of the normalized ratio of dEF/rSPh for sensing TTA-UC systems, based on PdTBP/BCP in 50% wt. carnauba wax/ varying oil composition. Black squares = RBO; red circles = AO; blue triangles = PEO. The other experimental parameters are the same as in Figure 4.

optically excited laser spot). For the identified optimal material composition (Figure 7 (a), the violet triangles) the ratio dEF/ rSPh is changed more than 15 times for a temperature interval of $\Delta T = 15\,^{\circ}C$–$45\,^{\circ}C$ centered around the temperature of interest ~36 °C: this allows for achieving of temperature sensitivity up to 100 mK, optically achieved in ambient environment, around the life-science relevant temperature.

4. Conclusion

In this study for the first time, all-optical temperature sensing in a natural wax-based organogel matrices via annihilation upconversion was realized. The sensing technique is based on ratiometric type signal registration that ensures significant independence of the data obtained on excitation intensity instabilities, local molecular concentration fluctuations and field-of-view variations. The identified matrix materials (natural wax/natural oils) are inherently biocompatible FDA-approved as food additives. The desired temperature sensitivity of better than 100 mK centered around the physiologically relevant temperature of 36 °C is warranted by using the process of triplet-triplet annihilation photon energy upconversion (TTA-UC) as a sensing mechanism. The TTA-UC system is effectively protected for more than 1000 s against oxygen-induced damages, allowing stable performance of this temperature-sensing system even in ambient environment without lost of sensitivity and applying the same calibration curve.

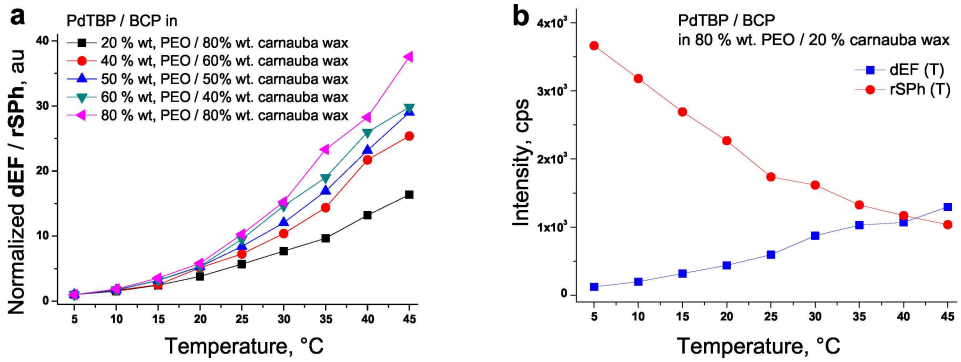

Figure 7. (a) Calibration curve based on temperature dependence of the normalized ratio of dEF/rSPh for sensing TTA-UC systems, based on PdTBP/BCP in varying compositions of carnauba wax/PEO; (b) Temperature dependence of the signals of dEF (blue squares) and rSPh (red circles) for the optimal TTA-UC system PdTBP/BCP in 80% wt. PEO/20% wt. carnauba wax. The other experimental parameters are the same as in Figure 4.

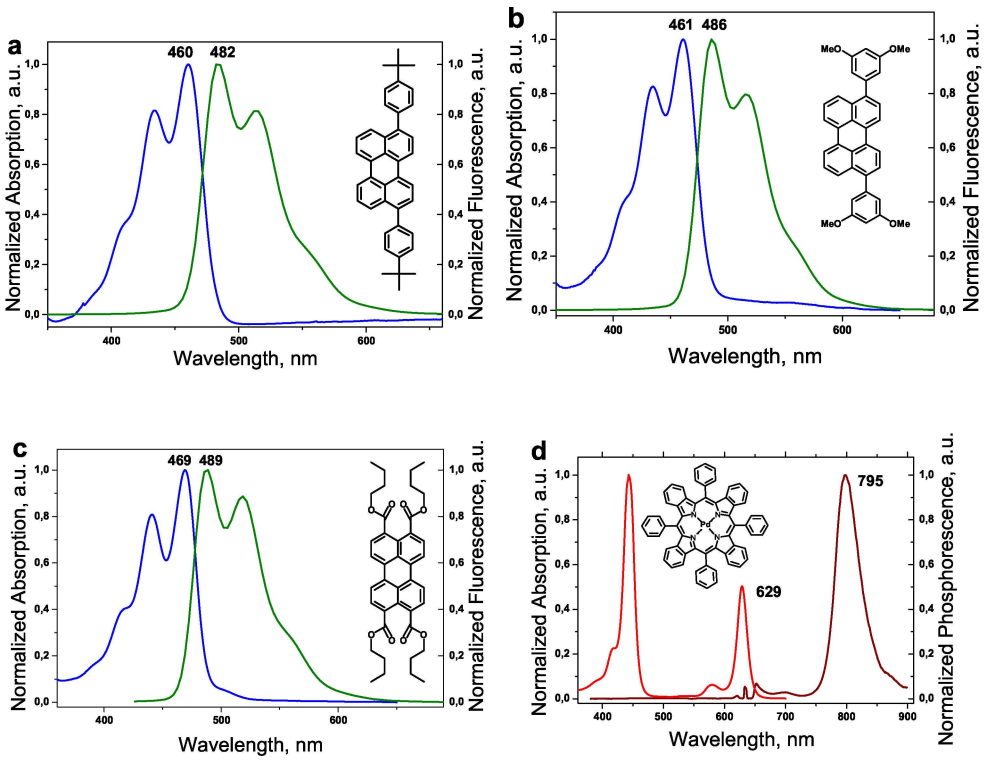

Figure 8. Absorption (blue line) and fluorescence (green line) spectra of emitters a, b and c. Insets: Structures of the emitters In (a) 3,10-Bis(4-*tert*-butylphenyl) = BDP; in (b) 3,9(10)-bis(3,5-dimethoxyphenyl) perylene = BMP; in (c) 3,4,9,10-tetra(butoxycarbonyl) = BCP. (d) Absorption (red line) and phosphorescence (brown line) spectra of the sensitizer. Inset: Structure of: *meso*-tetraphenyl-tetrabenzo[2,3]porphyrin palladium(II) = PdTBP.

Experimental Section

Materials

The chemical structures and absorption and emission spectra of upconversion dyes are shown in Figure 8. The chosen emitter molecules demonstrate almost identical fluorescence maxima ($\lambda =$ 482 nm for BDP; $\lambda = 486$ nm for BMP and $\lambda = 489$ nm for BCP): this fact minimizes the dependence of the process of TTA-UC on the energy position of the emitter singlet state. The molar concentration of the emitters is fixed to 2×10^{-4} M, kept the same for the entire optimization process.

The selection of the sensitizer was not optimized; for all measurements the sensitizer is PdTBP (Figure 8, d).[20] The molar concentration of the sensitizer is fixed to 1×10^{-5} M, kept the same for the entire optimization process.

Rice bran oil was purchased from TEA Natura (TEA Prodotti Naturali di Manzotti P., Italy), organic argan seed oil – from Primavera (Alnatura, Germany) and peanut oil – from Braendle (P. Braendle GmbH, Germany). Carnauba wax was purchased from Acros organics (USA) and bees wax – from Carl Roth (Carl Roth GmbH, Germany).

Sample Preparation

Toluene solutions of sensitizer (10^{-4} M, 100 μL) and emitter (10^{-3} M, 200 μL) were mixed at room temperature in 25 ml round-bottom flask and the solvent was evaporated to dryness under vacuum (40 °C, 74 mbar). The residue was dissolved in a vegetable oil (200/400/500/600/800 mg) and added to a molten wax (800/600/500/400/200 mg) in appropriate ratio, mixed at 100 °C for forming a homogeneous mixture. The samples were placed in glass tubes (VITROTUBES™, Hollow Rectangle Capillaries – N2540-50) with a thickness of 400 ± 10 μm and sealed with an epoxy.

Method

Luminescence spectra and kinetics were recorded by the home-made setup. The samples were excited with wavelength $\lambda_{exc} =$ 635 nm light beam from *cw*-diode laser. The excitation power was controlled using power meter PM 100D (Thorlabs, USA). For regular measurements, the excitation intensity was set to 20 mW cm^{-2}, laser spot diameter was $d = 1\times10^{-3}$ m. Sample was placed in a temperature-controlled holder. The holder temperature was controlled with a Peltier element by means of T-app computer program from Electron Dynamics Ltd. (Southampton, UK). The sample temperature additionally was controlled through a thermistor (PT100) attached on the top of the glass tube.

Acknowledgements

This work is performed under European Horizon 2020 research and innovation programme under grant agreement no. 732794 – project HYPOSENS. Open Access funding provided by the Max Planck Society.

Conflict of Interest

The authors declare no conflict of interest.

Keywords: biocompatibility · organogels · temperature sensing · triplet-triplet annihilation · upconversion

[1] H. Gudapati, M. Dey, I. Ozbolat, *Biomaterials.* **2016**, *102*, 20–42.
[2] I. Donderwinkel, J. C. M. van Hest, N. R. Cameron, *Polym. Chem.* **2017**, *8*, 4451–4471.
[3] H. S. Hwang, S. Kim, M. Singh, J. K. Winkler-Moser, S. X. Liu, *J. Am. Oil Chem. Soc.* **2012**, *89*, 639–647.
[4] P. R. Ogilby, *Chem. Soc. Rev.* **2010**, *39*, 8.
[5] T. T. Ruckh, H. A. Clark, *Anal. Chem.* **2014**, *86*, 3.
[6] X. Wang, O. S. Wolfbeis, *Chem. Soc. Rev.* **2014**, *43*, 10.
[7] X. Wang, O. S. Wolfbeis, R. J. Meier, *Chem. Soc. Rev.* **2013**, *42*, 19.
[8] D. B. Papkovsky, R. I. Dmitriev, *Chem. Soc. Rev.* **2013**, *42*, 22.
[9] K. Okabe, N. Inada, C. Gota, Y. Harada, T. Funatsu, S. Uchiyama, *Nat. Commun.* **2012**, *3*, 705.
[10] A. E. Albers, E. M. Chan, P. M. McBride, C. M. Ajo-Franklin, B. E. Cohen, B. A. Helms, *J. Am. Chem. Soc.* **2012**, *134*, 23.
[11] E. J. McLaurin, L. R. Bradshaw, D. R. Gamelin, *Chem. Mater.* **2013**, *25*, 8.
[12] J. Donner, S. Thompson, M. Kreuzer, G. Baffou, R. Quidant, *Nano Lett.* **2012**, *12*, 4.
[13] K. Landfester, Yu. Avlasesvich, D. Busko, F. Wurm, S. Balouchev, EP3072942-A1; WO2016150677-A1; EP3274420-A1; and US2018106785-A1, **2016**.
[14] a) H. Goudarzi, P. E. Keivanidis, *ACS Appl. Mater. Interfaces.* **2017**, *9*, 845–857; b) V. Gray, K. Moth-Poulsen, B. Albinsson, M. Abrahamsson, *Coord. Chem. Rev.* **2018**, *362*, 54–71; c) J. Pedrini, A. Monguzzi, *J. Photonics Energy* **2017**, *8*, 2; d) K. A. El Roz, F. N. Castellano, *Chem. Commun.* **2017**, *53*, 85; e) L. G. von Reventlow, M. Bremer, B. Ebenhoch, M. Gerken, T. W. Schmidt, A. Colsmann, *J. Mater. Chem. C.* **2018**, *6*, 15; f) T. Ogawa, M. Hosoyamada, B. Yurash, T. Q. Nguyen, N. Yanai, N. Kimizuka, *J. Am. Chem. Soc.* **2018**, *140*, 28; g) Y. Murakami, S. K. Das, Y. Himuro, S. Maeda, *Phys. Chem. Chem. Phys.* **2017**, *19*, 45. h) K. Katta, D. Busko, K. Landfester, S. Baluschev, R. Muñoz-Espı, *Isr. J. Chem.* **2018**, *58*, 1356–1362. i) J. Zhao, S. Ji, H. Guoa, *RSC Adv.* **2011**, *1*, 937–950. j) M. Hu, X. Zou, Q. Su, W. Yuan, C. Cao, Q. Wang, X. Zhu, W. Feng, F. Li, *Nat. Commun.* **2018** *9*, 2698.
[15] M. A. Filatov, E. Heinrich, D. Busko, I. Z. Ilieva, K. Landfester, S. Baluschev, *Phys. Chem. Chem. Phys.* **2015**, 17, 6501–6510.
[16] a) A. Loman, I. Gregor, Ch. Stutz, M. Mundb, J. Enderlein, *Photochem. Photobiol. Sci.* **2010**, *9*, 5; b) F. Fernandez-Alonso, F. J. Bermejo, S. E. McLain, J. F. C. Turner, J. J. Molaison, K. W. Herwig, *Phys. Rev. Lett.* **2007**, *98*, 077801; c) D. A. Turton, K. Wynne, *J. Phys. Chem. B.* **2014**, *118*, 17.
[17] a) M. A. Filatov, S. Baluschev, K. Landfester, *Chem. Soc. Rev.* **2016**, *45*, 4668–4689; b) S. Baluschev, K. Kata, Yu. Avlasevich, K. Landfester, *Mater. Horiz.* **2016**, *3*, 478–486.
[18] a) P. Goufo, H. Trindade, *Food Sci. Nutr.* **2014**, *2*, 2; b) A. E. Midaoui, Y. Haddad, R. Couture, *Nutrition.* **2016**, *32*; c) Eu. Choe, D. B. Min, *Compr. Rev. Food Sci. Food Saf.* **2006**, *5*; d) A. L. Petrou, P. L. Petrou, Th. Ntanos, A. Liapis, *Antioxidants.* **2018**, *7*, 35.
[19] A. R. Patel, M. Babaahmadi, A. Lesaffer, K. Dewettinck, *J. Agric. Food Chem.* **2015**, *63*, 19.
[20] a) M. Filatov, S. Baluschev, I. Ilieva, V. Enkelmann, T. Miteva, K. Landfester, S. Aleshchenkov, A. Cheprakov, *J. Org. Chem.* **2012**, *77*, 11119–11131; b) E. Heinrich, Yu. Avlasevich, K. Landfester, S. Baluschev, *J. Photonics Energy* **2018**, *8*, 022002–1/14.

Manuscript received: March 26, 2019
Revised manuscript received: May 16, 2019
Accepted manuscript online: May 25, 2019
Version of record online: June 12, 2019